Published in final edited form as:
Neurobiol Dis. 2008 October ; 32(1): 37–49. doi:10.1016/j.nbd.2008.06.012.

Localization and regional distribution of p23/TMP21 in the brain

Kulandaivelu S. Vetrivel[*,†], **Anitha Kodam**[*,§], **Ping Gong**[†], **Ying Chen**[†], **Angèle T. Parent**[†], **Satyabrata Kar**[§], and **Gopal Thinakaran**[†,**]

†*Departments of Neurobiology, Neurology, and Pathology, The University of Chicago, Chicago, IL 60637*

§*Centre for Prions and Protein Folding Diseases, Departments of Medicine (Neurology) and Psychiatry, University of Alberta, Edmonton, Alberta, T6G 2M8, Canada.*

Abstract

Sequential processing of amyloid precursor protein by β- and γ-secretases generates Alzheimer's disease (AD)-associated β-amyloid peptides. Recently it was reported that the transmembrane protein p23/TMP21 associates with γ-secretase, and negatively regulates β-amyloid production. Despite the link between p23 function and AD pathogenesis, the expression of p23 has not been examined in the brain. Here, we describe the detailed immunohistochemical characterization of p23 expression in rodent and human brain. We report that p23 is co-expressed with γ-secretase subunits in select neuronal cell populations in rodent brain. Interestingly, the steady-state level of p23 in the brain is high during embryonic development and then declines after birth. Furthermore, the steady-state p23 levels are reduced in the brains of individuals with AD. We conclude that p23 is expressed in neurons throughout the brain and the decline in p23 expression during postnatal development may significantly contribute to enhanced β-amyloid production in the adult brain.

Keywords

γ-secretase; nicastrin; presenilin; Alzheimer's disease; kainic acid; COP I

Introduction

Alzheimer's disease (AD) is pathologically characterized by the cerebral deposition of 39- to 43- amino acid β-amyloid peptides (Aβ) in the brain of afflicted individuals. Sequential proteolysis of amyloid precursor protein (APP) by β- and γ-secretases generate Aβ (Iwatsubo, 2004; Vassar, 2004). γ-secretase is a multimeric transmembrane protein complex containing presenilins (PS1 or PS2), nicastrin, APH-1 and PEN-2 as core subunits (Iwatsubo, 2004). Recently, p23 (also called TMP21) was identified as regulatory components of γ-secretase complex (Chen et al., 2006). p23 is a member of p24 family proteins, which are highly conserved type I transmembrane proteins involved in the coat protein (COP) I and II vesicle mediated cargo transport between ER and Golgi (Barlowe, 2000; Blum et al., 1999). p24 family proteins have proposed to regulate COP vesicle budding, ER quality control, organization of the Golgi apparatus, and the formation of tubular transport intermediates (Bethune et al., 2006; Simpson et al., 2006).

**Corresponding author: Gopal Thinakaran, Department of Neurobiology, The University of Chicago, Knapp R212, 924 E. 57th Street, Chicago, IL 60637. Tel. (773) 834-3752; Fax. (773) 834-3808; email: gopal@uchicago.edu .
*These authors contributed equally to this study

In mammals, members of the p24 family proteins function as homo and heterodimers (Jenne et al., 2002). A yeast *S. cerevisiae* mutant strain with deletion of all members of the p24 family was viable, and showed delay in the secretory pathway trafficking of select proteins (Belden and Barlowe, 2001; Springer et al., 2000). In the nematode *C. elegans* reducing the activity of the p24 family member SEL-9 increased the cell surface accumulation of a transport-defective mutants of the Notch homologues, GLP-1 and LIN-12 (Wen and Greenwald, 1999). In the fly *Drosophila*, loss of function mutations in p24 homologues reduced signaling associated with the TGF-β homologue, Dpp (Bartoszewski et al., 2004). Mice with homozygous disruption of p23 alleles exhibited early embryonic lethality, underscoring the physiological significance of p24 family proteins (Denzel et al., 2000).

An important link between p23 function and Aβ production was uncovered when it was found that p23 associates with γ-secretase complexes (Chen et al., 2006). Interestingly, reducing p23 expression results in increased γ-secretase cleavage of APP in intact cells and cell-free Aβ assays (Vetrivel et al., 2007). Moreover, knockdown of p23 expression conferred biosynthetic stability to nascent APP, allowing its efficient maturation, surface accumulation, and cleavage by α- and β-secretases (Vetrivel et al., 2007). These studies clearly establish that p23 is a negative modulator of Aβ production.

At present, there is no published report on the distribution and relative abundance of p23 in the central nervous system. Here, we performed detailed characterization on the localization of p23 in the adult rodent and human brain, and during the postnatal developmental stages in rodents. Our studies show that p23 is widely expressed in major brain areas, and co-localizes with γ-secretase core subunits PS1 and nicastrin in neurons. Interestingly, we show that steady-state p23 levels decline during postnatal development in rat and mouse brain. This age-related decline in p23 expression may be an intrinsic factor that significantly impacts on APP processing and Aβ burden in the aging nervous system.

Materials and methods

Animals and Autopsy Material

Sprague-Dawley rats obtained from Charles River (St Constant, Quebec) and B6C3F1/J mice obtained from The Jackson Laboratory (Bar Harbor, Maine) were used in the study. Animals were housed and maintained in accordance with the Institutional Policy on the handling and treatment of laboratory animals. Rat and mouse brain harvested during embryonic and postnatal developmental stages were prepared essentially as described previously (Thinakaran et al., 1996). For p23 immunostaining, well-characterized post-mortem human brain tissue samples from frontal cortex, hippocampus and cerebellum of AD (n = 8; age 78.3 ± 1.1 yrs; postmortem delay, 29 ± 6.4 hrs) and age-matched control (n = 6; age 72.8 ± 2.3 yrs; postmortem delay, 26.2 ± 4.2 hrs) were obtained from the Brain Bank of the Douglas Hospital Research Center, Montreal, Canada. Human brain tissues used for the Western blot analysis were obtained at autopsy, 1–10 h post-mortem, in the Brain Resource Center, The Johns Hopkins University School of Medicine. Brain tissue from seven controls free of any neurological diseases (age 30, 40, 59 [two individuals], 67, 75 and 86 years), and eight cases of sporadic AD (age 55, 56, 59, 61 [two individuals], 65, 76 and 80) were used. All cases of sporadic AD were pathologically confirmed by CERAD criteria and brains were stored at −70°C. Brain tissue from three patients with familial early-onset AD (FAD) carrying PS1 I143T mutation (age 36, 38 and 40 years) and from one patient with PS1 G384A mutation (age 40 years) were obtained at autopsy in the Born-Bunge Foundation (Cruts et al., 1995) and stored at −70°C.

Kainic acid administration

Thirty two adult male rats were injected intraperitoneally with kainic acid dissolved in normal saline (12 mg/kg) or equal volume of saline (0.2–0.25 ml) as described previously (Kar et al., 1997). Brains were harvested from control (n = 8), and kainic acid-injected rats at 12 h, 2 days or 12 days following the injection (n = 8 for each time point) and processed for Western blotting or immunohistochemistry as described below.

Cell culture

Primary mixed brain cultures were cultured from cortical tissue harvested from embryonic day 15 mouse embryos and maintained as described previously (Parent et al., 2005). For immunofluorescence studies, neurons were cultured on glass coverslips coated with 0.1% polyethylenimine in 15 mM borate buffer [pH 9]. HeLa cells stably expressing GFP-tagged N-acetylgalactosaminyltransferase-2 were cultured in Dulbecco's modified Eagle's medium supplemented with 10% fetal bovine serum. Mouse N2a neuroblastoma cells were maintained in 45% Dulbecco's modified Eagle's medium and 50% Opti-MEM (Invitrogen, Carlsbad, CA) supplemented with 5% fetal bovine serum.

Antibodies

The polyclonal p23 antiserum was raised against a synthetic peptide corresponding to N-terminal residues 32–57 of mouse p23 (Vetrivel et al., 2007) and affinity purified using an Ultralink Immobilization kit (Pierce, Rockford, IL). Rabbit polyclonal antisera $PS1_{NT}$ and α-PS1Loop, and polyclonal antiserum raised against PEN-2 have been described previously (Thinakaran et al., 1998; Vetrivel et al., 2004). Monoclonal Aβ antibody was a generous gift from Dr. S. Newman, Smith Kline Beecham Pharm, UK. The following antibodies were purchased from commercial sources: PS1 mAb (Affinity Bioreagents, Hornby, ON, Canada), polyclonal goat nicastrin antiserum (Santa Cruz Biotechnology Inc., Santa Cruz, CA); rabbit polyclonal APH-1 antibody (Zymed laboratories, San Francisco, CA); glial fibrillary acidic protein (GFAP) mAb, ED1 mAb (Serotec, Oxford, UK); GM130 mAb and N-Cadherin mAb (BD Transduction Laboratories, San Jose, CA); PSD-95 mAb (Upstate Biotech Inc., Charlettesville, VA) and GAPDH mAb (Abcam Inc., Cambridge, MA), and β-actin mAb and synaptophysin mAb (Sigma-Aldrich, Mississauga, ON, Canada). Donkey anti-goat Texas red, donkey anti-rabbit FITC and CY3-conjugated secondary antibodies were from Jackson Immunoresearch (West Grove, PA), and Alexa 488- and 555-conjugated secondary antibodies were from Invitrogen (Carlsbad, CA).

Protein Analyses

Total protein lysates from post-mortem human brain tissue and mouse brain harvested during embryonic and postnatal developmental stages were prepared essentially as described previously (Thinakaran et al., 1996). Brain regions of interest were dissected from six normal adult rats and four rats from each of the postnatal developmental stages P1, P7 and P21. Tissues were homogenized in ice-cold RIPA-lysis buffer [20 mM Tris HCl (pH 8), 150 mM NaCl, 0.1% SDS, 1 mM EDTA, 1% Igepal CA-630, 50 mM NaF, 1 mM $NaVO_3$, 10 μg/ml leupeptin and 10 μg/ml aprotinin]. Similarly, hippocampal regions from control (n = 4) and kainic acid treated rats (4 animals from each time point) were dissected out and homogenized in RIPA-lysis buffer. Proteins were separated in 4–12% or 4–20% NuPAGE gels (Invitrogen, Burlington, Canada) and immunoblotted with 1:1000 dilution of p23 antibody or appropriate dilutions of the loading control and marker antibodies. For peptide competition, antibodies were preincubated with 40 μg/ml of an unrelated peptide (control) or the p23 peptide immunogen at 4°C overnight prior to incubation with the blot containing N2a total protein lysate. N2a cells grown to subconfluency were lysed in 1% CHAPSO and used for co-immunoprecipitation as described previously (Chen et al., 2006). Polyclonal antibody

STC261 raised against stanniocalcin 2 (Ito et al., 2004) was used as negative control to establish specificity for the co-immunoprecipitation. For quantification, the immunoblots were developed by chemiluminescence method and exposed to X-ray films for various lengths of time to ensure that the signals are not saturated. Optimal exposures were quantified using standard densitometry and a calibration step tablet was used to convert raw optical densities to relative fold difference in signal intensity essentially as described (http://rsb.info.nih.gov/ij/docs/examples/calibration/) using Metamorph software (Molecular Devices Corporation, Downingtown, PA). Normalized signal intensities were compared between sporadic AD (mean age 64.13 ± 3.2) and FAD cases (mean age 38.5 ± 1) and their respective age-matched controls (older controls mean age 69.2 ± 5.1 and young controls mean age 35 ± 5, respectively). The data are presented as mean ± S.E.M, and statistical significance was analyzed by *t*-tests.

Immunohistochemistry

Eight normal adult rats and 16 rats from kainic acid treated experimental group (i.e., 4 saline-treated control and 4 rats from each time-point) were deeply anesthetized prior to perfusion with phosphate-buffered saline (PBS) [pH 7.2] followed by 4% paraformaldehyde. Similarly, four postnatal rats from each stages of development (i.e., P1, P7 and P21) were anesthetized and perfused with PBS followed by 4% paraformaldehyde or Bouin's solution. After perfusion, brains were post-fixed overnight in the same fixative and then stored at 4°C in 30% PBS/sucrose. Human brain tissues were immersion fixed in formalin and then stored in 30% PBS/sucrose. Brain tissues were coronally sectioned (20 and 40 μm) on a cryostat and then processed for either enzyme-linked immunoperoxidase or double immunofluorescence method as described earlier (Kodam et al., 2008). For immunoperoxidase procedure, sections were washed with PBS, treated with 1% hydrogen peroxide for 30 minutes, treated with 10 mM sodium citrate buffer and autoclaved for 20 min. Sections were then incubated overnight with p23 antisera (1:1000), exposed to avidin-biotin reagents for 1 hr at room temperature and then developed using glucose-oxidase-diaminobenzidine tetrahydrochloride-nickel enhancement method (Kodam et al., 2008). The specificity of the p23 antibody was determined by omission of the primary antibody, peptide competition (see above), or by incubating the sections with preimmune serum. Immunostained sections were examined under a Zeiss Axioskop-2 microscope and the photomicrographs were taken with a Nikon 200 digital camera and exported to the Adobe Photoshop 6.0 program for further processing. The rat brain atlas of Paxinos and Watson (Paxinos and Watson, 1986) was used to define and name anatomical structures.

Immunofluorescence labeling

HeLa cells cultured on poly-L-lysine coated glass coverslips were fixed with 4% paraformaldehyde in PBS [pH 7.4] for 20 min and permeabilized using PBS containing 0.5% SDS, 5% β-mercaptoethanol and 10% fetal bovine serum as described (Blum et al., 1999). Neuronal cultures were fixed and permeabilized as above for 15 min. Cells on coverslips were blocked with PBS containing 3% BSA and incubated for overnight at 4°C with affinity-purified p23 antibody (1:500) and anti-GM130 antibody (1:1000) diluted in PBS containing 0.2% Tween-20 and 3% BSA, followed by incubation with Alexa 488- and 555-conjugated secondary antibodies (1:500). Images were acquired as 200 nm z-stacks on a motorized Nikon TE2000 microscope with Cascade II:512 CCD camera (Photometrics, Tucson, AZ) using 100X 1.45 NA Plan-Apochromat oil immersion objective. Image stacks were deconvolved using Huygens software (Scientific Volume Imaging BV, The Netherlands) and processed using Metamorph software (Molecular Devices Corporation, Downingtown, PA). Confocal images of neuronal cultures were acquired with a 100X 1.45 NA Plan-Apochromat oil immersion objective on a Zeiss laser-scanning microscope (Pascal 5) and processed as above.

Adult rat brain sections (20 μm) were incubated overnight at room temperature with p23 antiserum (1:300) in combination with either goat anti-nicastrin (1:50) or mouse anti-PS1 antibodies. In the case of kainic acid-treated animals, sections were incubated with p23 antiserum along with either anti-GFAP (1:500) or anti-ED1 (1:50) antibodies. Human AD brain sections were treated with 87% formic acid for 7 min prior to incubation with p23 antiserum and Aβ antibody (1:500). Sections were incubated with Texas Red-, FITC-, or Cy3-conjugated secondary antibodies (1:200) and mounted using Vectashield mounting medium (Vector Laboratories, Burlingame, CA). Sections were examined under a Zeiss Axioskop-2 fluorescence microscope and the photomicrographs were taken with a Nikon 200 digital camera and exported to the Adobe Photoshop for further processing.

Results

Immunoblot analysis of p23 expression in neuroblastoma cells and rat brain

Recent studies indicate that p23 functions as a negative modulator of Aβ production in addition to its documented role in regulating vesicular transport between the ER and Golgi (Chen et al., 2006; Vetrivel et al., 2007). Since the localization of p23 in the central nervous system has never been examined, we set out to characterize the expression and distribution of p23 in rat and mouse as well as human brains using immunoblotting and immunohistochemical studies. We first affinity purified a rabbit polyclonal antiserum raised against a synthetic peptide corresponding to the N-terminal luminal residues 32–57 of mouse p23 (Vetrivel et al., 2007). To demonstrate the specificity of the purified antibody, we performed peptide competition studies using a non-specific synthetic peptide (control) or p23 peptide immunogen (described above). As expected, p23 antibody preincubated with the control peptide reacted with a single protein with molecular size of 23 kDa; this reactivity was completely eliminated when the antibody was preincubated with the p23 peptide immunogen (Fig. 1A). Previously Chen et al. reported that p23 was co-isolated with γ-secretase complex subunits (Chen et al., 2006). In accordance with this study, endogenous γ-secretase complexes co-immunoprecipitated using antibodies against PS1 from 1% CHAPSO lysates of N2a cells contained small amounts of endogenous p23 in addition to the four core subunits (PS1-derived N- and C-terminal fragments, mature nicastrin, PEN-2 and APH-1) (Fig. 1B). Then, we characterized the specificity of p23 antibody and its ability to recognize endogenous p23 in different regions of the adult rat brain using immunoblotting. As shown in Fig 1C, the antiserum recognized a single major protein with an apparent molecular weight of 23 kDa, corresponding to the p23. The p23 protein was expressed all major regions of the adult rat brain including the septum, striatum, cortex, hippocampus, amygdala, thalamus, hypothalamus, cerebellum and brainstem (Fig. 1C).

Subcellular localization of p23

In cultured non-neuronal cells p23 predominantly resides in Cis-Golgi cisternae and adjacent tubulovesicular membranes (Blum et al., 1999; Rojo et al., 1997). In agreement with these previous findings, the p23 antibody employed in our investigation stained the Golgi apparatus in HeLa cells, where it colocalizes with the Golgi-resident enzyme N-acetylgalactosaminyltransferase-2 (Fig. 2A). In addition to the predominant Golgi localization, p23 staining of small vesicles is also observed. Next, we examined the localization of p23 in primary mouse cortical neuronal cultures. Consistent with p23 localization in non-neuronal cells, we observed perinuclear staining for p23 mainly in the cell body of neurons. Double immunofluorescence staining with the cis-Golgi marker, GM130 revealed co-localization of p23 with GM130 in cultured mouse cortical neurons (Fig. 2B). Similarly, in cultured astrocytes p23 staining was found in the Golgi apparatus where it co-localized with GM130 (Fig. 2C). These findings indicate that the main function of p23 in neuronal cells may be similar to that of non-neuronal cells, i.e., the regulation of biosynthetic protein transport.

p23 immunoreactivity in the adult rat brain

Having established the specificity of the p23 antibody, we analyzed the localization of p23 in the brain using frozen sections prepared from the adult rat brain. Results showed that p23 immunoreactivity is widely distributed throughout the adult rat brain including the basal forebrain, basal ganglia, cerebral cortex, hippocampus, thalamus, hypothalamus, cerebellum, and brainstem (Fig. 3 and Fig 4). We observed region-specific differences in p23 immunoreactivity, which is evident mostly in neurons and fibers but not in glial cells. The specificity of the p23 immunostaining was further established by using preimmune serum, which failed to show specific staining in any given region of the brain (Fig. 4F). In the following sections, we describe the overall distribution profile of p23 immunoreactivity observed in specific regions of the brain.

Basal forebrain and basal ganglia—p23 immunoreactivity was evident in all sub regions of the basal forebrain including the septum, diagonal band complex and nucleus baslis of Meynert. In septal nuclei, several multipolar cells were moderately labeled, whereas in the diagonal band complex, some intensely labeled neurons were found along with some weakly labeled neurons (Fig. 3A). A number of rather moderately labeled neurons were also encountered in the bed nucleus of the stria terminalis, nucleus basalis of Meynert, globus pallidus, entopeduncular nucleus and ventral pallidum (Fig. 3B). A subset of p23-positive multipolar neurons, located between unstained myelinated fascicles was found scattered throughout the caudate putamen (Fig. 3C).

Cerebral cortex—p23 immunoreactive neurons were detected in most layers of the neocortex with varying degrees of staining intensity i.e., labeling was high in layers II–VI and relatively low in layer I (Figs. 3D and E). The laminar distribution of p23 labeled neurons was most striking in the cingulate cortex and the frontoparietal cortex than in other cortical regions. A number of moderately stained smaller multipolar neurons intermingled with strongly labeled neurons were visible in layers II–III, whereas most of the pyramidal neurons located in layers IV and V were intensely labeled with vertically oriented apical dendrites (Fig. 3E). Some scattered multipolar neurons with moderate somatodendritic labeling were evident in layer VI of the cortex. In the piriform cortex, intensely labeled neurons were apparent in both the pyramidal and polymorphic layers, intermingled with some weakly labeled neurons.

Hippocampus—The hippocampal formation showed some of the most intense and abundant p23 immunoreactivity in the brain (Fig. 3F). Strong labeling was apparent in the CA1–CA3 pyramidal cell layer located within the Ammon's horn. Virtually all pyramidal neurons and their apical dendrites, which were often seen extending into the adjacent *stratum radiatum* layer, displayed intense p23 labeling (Fig. 3G). Outside the pyramidal layer, few medium-sized, multipolar or fusiform p23-immunoreactive neurons were scattered throughout the *strata oriens* and *stratum radiatum* but not in *lacunosum moleculare*. Within the dentate gyrus, granule cell somata were strongly labeled. Large, polymorphic, heavily stained neurons were also present in the hilus (Fig. 3H), whereas very little p23 immunoreactivity was observed in the adjacent molecular layer.

Hypothalamus and Thalamus—A rather strong p23 neuronal labeling was observed in the supraoptic and paraventricular hypothalamic nuclei (Fig. 3I and J), whereas neurons located in the ventromedial nucleus, dorsolateral hypothalamic areas and arcuate nucleus exhibited moderate labeling. A number of medium-sized p23-immunostained neurons were observed throughout the thalamus particularly in ventral and lateral portions (Fig. 4A) and in the habenular nucleus.

Amygdala—A number of moderately labeled p23-immunoreactive cell bodies were evident in the cortical, medial and basolateral amygdaloid nuclei (Fig. 4B). Some multipolar cells exhibiting rather weak immunoreactivity were apparent in the anterior amygdaloid area and central amygdaloid nucleus. In the amygdaloid nuclei, p23 immunoreactivity was found predominantly associated with cell bodies (see Fig. 4B inset).

Midbrain—Moderate p23 labeling was observed in the cell bodies located in the superficial gray layers of the superior colliculus and in the central gray matter. The substantia nigra pars reticulata was characterized by multipolar neurons with moderate to weak p23 immunoreactivity. Neurons of the red and oculomotor nuclei displayed rather intense immunoreactivity. Moderately labeled p23 positive neurons were also apparent in the intermediate gray layer of superior colliculus and mesencephalic trigeminal nucleus.

Brainstem—Strong p23 immunoreactivity was apparent at all levels of the brainstem. A number of multipolar p23-immunoreactive neurons were encountered in the pontine reticular nucleus, inferior colliculus, abducens nucleus and reticulotegmental nucleus of pons (Fig. 4C). Intense labeling was also evident in the motor trigeminal nucleus, pontine nucleus and in the vestibular as well as facial nuclei (Fig. 4D). Additionally, a population of large multipolar process bearing neurons was encountered in the dorsal raphe nucleus and in dorsal as well as ventral parts of the cochlear nucleus.

Cerebellum—Intense p23 immunoreactivity was evident throughout the cerebellum. In the cortex, Purkinje cells were heavily stained and often seen in continuity with their stained dendritic shafts extending into the molecular layer (Fig. 4E). The granule cells exhibited rather weak staining, whereas a number of deep cerebellar nuclei showed numerous moderate to weakly labeled p23-positive cell bodies and dendrites.

Co-expression of p23 with PS1 and nicastrin in the adult rat brain

Recently we characterized the regional distribution of γ-secretase subunits nicastrin and PS1 in rodent brain and found that both proteins were co-expressed in select neuronal populations throughout the brain (Kodam et al., 2008). To further extend the findings described above, and provide a cellular basis of functional interrelationship between p23 and the γ-secretase complex, we performed double immunofluorescence labeling of p23 with nicastrin or PS1 in sections from different brain regions. Our results clearly showed that p23 is co-expressed with nicastrin- and PS1-positive neurons in cerebral cortex (Fig. 5A–C, Fig. 6A–C), hippocampus (Fig. 5D–F, Fig. 6D–F), brainstem motor nuclei (Fig. 5G–I, Fig. 6G–I) and cerebellar Purkinje cells (Fig. 5J–L, Fig. 6J–L). It is apparent from these results that p23 colocalizes with nicastrin and PS1 in neurons located in the aforementioned brain regions.

p23 immunoreactivity in kainic acid-treated rat brain

Earlier studies have shown that administration of kainic acid, an agonist for a subtype of ionotropic glutamate receptor, can induce extensive degeneration of hippocampal pyramidal neurons accompanied by hypertrophy of astrocytes and microglial cells (Nadler et al., 1980). To determine whether p23 immunoreactivity is altered following degeneration of neurons in the hippocampus, we evaluated the levels and cellular distribution of p23 following systemic administration of kainic acid into the adult rat. Our Western blotting data showed that steady-state levels of p23 in the hippocampus were not significantly altered at 12 h, 2 d or 12 d following kainic acid administration compared to controls (data not shown). However, at the cellular level we observed that expression of p23 is induced in the reactive glial cells in a time-dependent manner concomitant with a decrease in expression in the pyramidal neurons, which undergo degeneration following the administration of kainic acid (Fig. 7A–F). Our double labeling experiments further revealed that expression of p23 was evident in GFAP-labeled

reactive astrocytes 12 d after kainic acid treatment, but not detectible in ED1-positive microglia (Fig. 7G).

p23 immunostaining in human AD brains

We tuned our attention to p23 expression in human brain and performed immunostaining of brain tissue from patients with AD and age-matched controls. We found that p23 immunoreactivity is widely distributed throughout the frontal cortex, hippocampus and cerebellum of control and AD brains (Fig. 8A–O). In control brains, p23 immunoreactivity was detected principally in neuronal cell bodies and their process but not in glial cells. In the frontal cortex, p23-immunoreactive neurons were evident in all layers except layer I, but the staining intensity varied considerably between layers II–VI. A number of moderately stained multipolar neurons were visible in layers II–III, whereas pyramidal neurons with apical dendrites were strongly labeled in layers IV and V of the cortex. Layer VI is characterized by some scattered multipolar neurons with moderate somatodendritic labeling (Fig. 8A–B). The hippocampal formation showed rather intense p23 immunoreactivity, primarily in neuronal soma and fibers. Within the Ammon's horn, strong labeling was apparent in the CA1–CA4 pyramidal cell layer, whereas some pyramidal neurons were found to extend their apical dendrites into the adjacent *stratum radiatum* layer. Within the dentate gyrus, granule cell soma exhibited rather weak labeling. Large, intensely labeled polymorphic neurons were present in the hilus, whereas little or no p23 immunoreactivity was evident in the molecular layer (Fig. 8E, F, H). In the cerebellum, p23 immunoreactivity was evident primarily in Purkinje cells and their dendritic shafts, which often extended into the adjacent molecular layer (Fig. 8J). The granule cells and some scattered cell bodies in the molecular layer of the cerebellum exhibited moderate p23 staining.

In AD brains, a number of Aβ-containing neuritic plaques were evident in both the cortex and hippocampus (Fig. 8L and N). As observed in control brains, p23 immunoreactivity is evident in neurons of the frontal cortex (Fig. 8C, D), hippocampus (Fig. 8G, I) and cerebellum (Fig. 8K) of the AD brain. No striking difference in the p23 immunoreactivity was apparent in the cerebellum of the AD brain compared to age-matched controls. However, the labeling of surviving pyramidal neurons in the frontal cortex and hippocampal regions of the AD brain appeared to be less intense than control brains (Fig. 8F, G). We performed double labeling experiments using p23 and Aβ antibodies, and found that p23 labeling is mainly associated with neuronal cell bodies, and only occasionally overlapped with Aβ staining in neuritic plaques in the frontal cortex and hippocampal regions (Fig. 8L–O).

To quantitatively assess the levels of p23 in brains of patients with AD and age-matched controls, we performed Western blot analysis of brain homogenates using antibodies against p23 and γ-secretase subunits nicastrin and PS1. Brain cortical tissue from eight sporadic AD cases, four FAD cases from two Belgian AD pedigrees with mutations in *PSEN1* gene [I143T or G384A substitution; (Cruts et al., 1995)] and seven age-matched controls were examined. In all brain extracts examined, p23 antiserum reacted with ~23 kDa polypeptide. The blots were sequentially reprobed with nicastrin, PS1 and GAPDH antibodies. Quantification of immunoblot signals (normalized to GAPDH levels, which serves as the loading control) revealed a significant decrease in the levels of p23 between age-matched controls and AD cases, whereas the levels of γ-secretase subunits nicastrin and PS1 (not shown) remained unchanged between control and AD cases (Table 1). When p23 signals were normalized to that of nicastrin, it is apparent that there is a modest, but significant difference in the levels of p23 between SAD cases relative to age-matched older controls (35.5 ± 15.4% decrease in SAD cases; $p < 0.05$). Similarly, when FAD cases were compared to young age-matched controls, there was a significant decrease in the levels of p23 relative to nicastrin (65.8 ± 18.9% decrease in FAD cases; $p < 0.03$) (Fig. 9C). Thus, p23 is expressed in neurons in human brain, and in

the cortex there is a decrease in the steady-state levels of p23 relative to γ-secretase subunits in the brains of individuals afflicted with SAD and FAD.

Postnatal regulation of p23 expression in the brain

Subunits of the γ-secretase are expressed in embryonic brain and intramembranous γ-secretase cleavage of substrates such as Notch receptors and deleted in colorectal cancer (DCC) is essential for signaling during neuronal development (Vetrivel et al., 2006). To determine p23 distribution profile during postnatal development of the brain, we performed immunocytochemical analyses of the cortex, hippocampus, cerebellum and brainstem obtained from P1, P7, P21 and adult brains. At the cellular level, we found that p23 immunoreactivity is widely distributed at all stages of the postnatal developing brains. However, at the early stages of development p23 immunoreactivity was restricted primarily to neuronal cell bodies, whereas at later stages (i.e., P21 and adult) immunoreactivity was apparent not only in the cell bodies but also in dendrites/neuropil of all brain regions (Fig. 10 A–C). Moreover, we noted that the intensity of p23 labeling decreased gradually during the course of postnatal development.

To determine whether p23 expression is regulated during postnatal development, we performed immunoblotting of mouse brain homogenates prepared from different developmental stages. We found high levels of p23 expression in embryonic mouse brain, but the steady state p23 levels gradually declined after birth to the lower adult level (Fig. 10D and E). In contrast, expression of the presynaptic protein synaptophysin and post-synaptic protein PSD-95 is very low in embryonic brain and increases markedly after birth. N-cadherin expression is similar during embryonic and postnatal developmental stages and serves as a loading control (Fig. 10D and E). The postnatal decrease in the steady-state level of p23 was further confirmed by immunoblot analysis of cortex and hippocampal homogenates of rat brain harvested at P1, P7 and P21 (data not shown). Understanding the functional significance of the decline in p23 expression to amyloid burden in the aging brain remains an active subject of our future investigation.

Discussion

The p24 family proteins play an important role in vesicular trafficking in the early secretory pathway (Bethune et al., 2006). Homozygous deletion of p23 resulted in early embryonic lethality of mouse embryos signifying the physiological importance of p23 protein during mammalian embryonic development (Denzel et al., 2000). The recent findings that p23 co-purifies with γ-secretase complex, and modulates APP trafficking and Aβ production illustrate a potentially critical function of p23 in AD pathogenesis (Chen et al., 2006; Vetrivel et al., 2007). Despite the physiological significance of p23 function, knowledge is lacking on p23 expression in the central nervous system. The present study was undertaken to analyze cellular expression and distribution of p23 in rodent and human brain, and in this report we describe the first comprehensive analysis of cellular distribution as well as postnatal expression of p23 in the brain.

Mammalian p24 family proteins exist as monomers and dimers in the endoplasmic reticulum, Golgi, and the intermediate compartments (Jenne et al., 2002). Therefore, it was surprising that p23 was identified as a γ-secretase complex component by affinity purification of PS1-associated proteins (Chen et al., 2006). We independently confirmed endogenous p23 association with PS1 complex by co-immunoprecipitation of endogenous γ-secretase subunits in mouse N2a neuroblastoma cells using an antibody raised against the N-terminal residues 1–65 of PS1 (Thinakaran et al., 1998). Notably, the abundance of p23 in PS1 complex relative to the input in our experiments raises the possibility that p23 associates with only a subset of γ-secretase complexes (Fig. 1B). This is an important observation because previous siRNA

knockdown studies indicate that p23 is a negative modulator of Aβ production (Chen et al., 2006; Vetrivel et al., 2007). Thus, it appears that Aβ production by p23 association with γ-secretase may be regulated by the abundance of "free" p23 that is not present as a heterodimer with other members of the p24 family.

Our Western blot analysis revealed that p23 is expressed in all major areas in rat brain. However, immunohistochemical analysis showed clear variation in the intensity of staining in different regions of the brain as well as labeling of individual cells. At the cellular level, there is intense staining in the neuronal populations than in glial cells. Strong staining was evident in hippocampus, neocortex and more importantly pyramidal neuronal cell populations. Some of these regions are most vulnerable to pathological changes associated with AD. Co-localization of p23 with PS1 and nicastrin, two core components of γ-secretase, in neuronal populations of the cortex and hippocampus indicate that subset of γ-secretase complexes in these neurons could possibly contain p23 associated with them. Similarly, p23 immunostaining pattern in human brain matched with that of rat brain, and showed intense staining in hippocampal neuronal populations. Immunoblot analysis of p23 expression showed reduced signals for p23 in brain tissue from sporadic AD and FAD brains bearing *PSEN1* I143T and G384A mutations, relative to respective old and young age-matched controls, respectively (Fig. 9 and Table 1). The observation that the levels of p23 are significantly reduced relative to γ-secretase subunits in AD tissue indicates that this decrease in p23 levels may have functional importance in the modulation of APP processing by the γ-secretase similar to what has been shown in cultured cell lines (Chen et al., 2006;Vetrivel et al., 2007). Thus, we suggest that the balance between the levels of p23 and γ-secretase is one of the factors that influence the extent of amyloid burden in the brains of individuals with AD.

Immunofluorescence analysis of primary neuronal cultures revealed predominant localization of p23 with the Golgi marker GM130 in neurons (Fig. 2). Restricted localization of p23 to Golgi membranes is expected based on previous studies on p23 in non-neuronal cells such as HeLa (Blum et al., 1999). Interestingly, p23 immunoreactivity is prominently observed in neuronal soma as well as apical dendrites of pyramidal neurons in the cortex and hippocampus, and the dendrites of cerebellar Purkinje neurons (Fig. 3 and Fig. 4). Based on the co-localization of p23 with GM130 in the dendrites of primary cortical neurons, the dendritic staining in brain tissue likely represents localization of p23 in Golgi outposts that are known to partition into larger dendrites in neurons (Horton et al., 2005). As a major function for p23 is to regulate vesicular trafficking in the early secretory pathway, it remains to be determined whether p23-bound γ-secretase complexes are selectively targeted to Golgi outposts in the dendrites. Moreover, the lack of p23 staining in axons is noteworthy because APP C-terminal fragments containing the entire Aβ sequence are transported in the fast component of anterograde transport of neurons in the central nervous system (Buxbaum et al., 1998), and are thought to be cleaved by γ-secretase at or *en route* to the neuronal terminals to release Aβ near synapses. Based on our findings, it is unlikely that the subset of γ-secretase in the axonal compartment can be negatively regulated by p23.

Previous studies suggest a general role for p23 in the recruitment of the small GTPase ADP-ribosylation factor-1 to the donor Golgi membrane during COP I-vesicle formation, which is a highly conserved process in eukaryotic cells (Gommel et al., 2001). Therefore it was surprising that p23 immunohistochemical staining was only weakly detected in astrocytes in rat or human brain sections. Nevertheless, we were able to observe strong p23 labeling in cultured astrocytes, where the staining co-localized with the Golgi marker GM130 (Fig. 2). Furthermore, kainic acid induced neurodegeneration selectively elevated p23 expression in astrocytes but not in microglial cells in rat brain. It would be interesting to determine whether p23 function in the astrocytes is involved in neurodegeneration or protection against seizure-induced brain damage. It should be noted that this is only a preliminary observation and closer

scrutiny on the mechanism of astrocytic upregulation of p23 awaits further detailed investigation in the future. Nevertheless, the results described above show that p23 is expressed in neuronal populations throughout the brain, and under certain conditions can be upregulated in astrocytes.

Finally, our studies also reveal remarkable postnatal developmental changes in p23 expression in the brain. We found that the steady-state level of p23 was high during the early stages of embryonic development, and then declined to the lower adult levels few months after birth. Notably, p23 expression markedly declines in the first few weeks after birth, at a time when presynaptic and post-synaptic proteins begin to express in the brain. Moreover, this age-dependent decrease in p23 expression is particularly interesting, and significant with reference to Aβ burden in the brain because of the negative regulation of Aβ production by p23 (Chen et al., 2006; Vetrivel et al., 2007). As described above, successful interaction of p23 with γ-secretase depends on the abundance of p23 that is not complexed with other p24 family proteins. We suggest that the high abundance of p23 during the early stages of development likely allows p23 to negatively modulate Aβ production by association with the γ-secretase, thus keeping Aβ levels under tight control in young animals. In contrast, as the animal age, the decline in the steady-state level of p23 could markedly influence the availability of free p23 to interact with the γ-secretase complex, thus relieving p23-mediated negative control of Aβ production. We are in the process of testing the above hypothesis by generating p23 transgenic mice.

Abbreviations

Aβ, β-amyloid; AD, Alzheimer's disease; APP, amyloid precursor protein; COP, Coat protein; FAD, familial early-onset AD; GFAP, glial fibrillary acidic protein; PBS, phosphate-buffered saline; PS, presenilin(s).

Acknowledgements

We thank Ms. Danielle Cécyre and the Douglas Hospital Research Centre Brain Bank, Dr. Juan Troncoso at the Brain Resource Center in The Johns Hopkins University School of Medicine, and Drs. Lydia Hendriks and Christine Van Broeckhoven at the Born-Bunge Foundation for providing human tissue, and Ms. Natalie Barnes for technical assistance. This work is supported by NIH grants to GT (AG021495 and AG019070) and ATP (NS055223), grants from the Alzheimer's Association to ATP and KSV (IIRG-06-26148 and NIRG-05-14427), and a grant from Canadian Institutes of Health Research to SK.

References

Barlowe C. Traffic COPs of the early secretory pathway. Traffic 2000;1:371–377. [PubMed: 11208122]

Bartoszewski S, Luschnig S, Desjeux I, Grosshans J, Nusslein-Volhard C. Drosophila p24 homologues eclair and baiser are necessary for the activity of the maternally expressed Tkv receptor during early embryogenesis. Mech Dev 2004;121:1259–1273. [PubMed: 15327786]

Belden WJ, Barlowe C. Deletion of yeast p24 genes activates the unfolded protein response. Mol Biol Cell 2001;12:957–969. [PubMed: 11294899]

Bethune J, Wieland F, Moelleken J. COPI-mediated Transport. J Membr Biol 2006;211:65–79. [PubMed: 17041781]

Blum R, Pfeiffer F, Feick P, Nastainczyk W, Kohler B, Schafer KH, Schulz I. Intracellular localization and in vivo trafficking of p24A and p23. J Cell Sci 1999;112(Pt 4):537–548. [PubMed: 9914165]

Buxbaum JD, Thinakaran G, Koliatsos V, O'Callahan J, Slunt HH, Price DL, Sisodia SS. Alzheimer amyloid protein precursor in the rat hippocampus: transport and processing through the perforant path. J Neurosci 1998;18:9629–9637. [PubMed: 9822724]

Chen F, Hasegawa H, Schmitt-Ulms G, Kawarai T, Bohm C, Katayama T, Gu Y, Sanjo N, Glista M, Rogaeva E, Wakutani Y, Pardossi-Piquard R, Ruan X, Tandon A, Checler F, Marambaud P, Hansen

K, Westaway D, St George-Hyslop P, Fraser P. TMP21 is a presenilin complex component that modulates γ-secretase but not ε-secretase activity. Nature 2006;440:1208–1212. [PubMed: 16641999]

Cruts M, Backhovens H, Wang SY, Gassen GV, Theuns J, De Jonghe CD, Wehnert A, De Voecht J, De Winter G, Cras P, et al. Molecular genetic analysis of familial early-onset Alzheimer's disease linked to chromosome 14q24.3. Hum Mol Genet 1995;4:2363–2371. [PubMed: 8634711]

Denzel A, Otto F, Girod A, Pepperkok R, Watson R, Rosewell I, Bergeron JJ, Solari RC, Owen MJ. The p24 family member p23 is required for early embryonic development. Curr Biol 2000;10:55–58. [PubMed: 10660306]

Gommel DU, Memon AR, Heiss A, Lottspeich F, Pfannstiel J, Lechner J, Reinhard C, Helms JB, Nickel W, Wieland FT. Recruitment to Golgi membranes of ADP-ribosylation factor 1 is mediated by the cytoplasmic domain of p23. Embo J 2001;20:6751–6760. [PubMed: 11726511]

Horton AC, Racz B, Monson EE, Lin AL, Weinberg RJ, Ehlers MD. Polarized secretory trafficking directs cargo for asymmetric dendrite growth and morphogenesis. Neuron 2005;48:757–771. [PubMed: 16337914]

Ito D, Walker JR, Thompson CS, Moroz I, Lin W, Veselits ML, Hakim AM, Fienberg AA, Thinakaran G. Characterization of stanniocalcin 2, a novel target of the mammalian unfolded protein response with cytoprotective properties. Mol Cell Biol 2004;24:9456–9469. [PubMed: 15485913]

Iwatsubo T. The γ-secretase complex: machinery for intramembrane proteolysis. Curr Opin Neurobiol 2004;14:379–383. [PubMed: 15194119]

Jenne N, Frey K, Brugger B, Wieland FT. Oligomeric state and stoichiometry of p24 proteins in the early secretory pathway. J Biol Chem 2002;277:46504–46511. [PubMed: 12237308]

Kar S, Seto D, Dore S, Chabot JG, Quirion R. Systemic administration of kainic acid induces selective time dependent decrease in [125I]insulin-like growth factor I, [125I]insulin-like growth factor II and [125I]insulin receptor binding sites in adult rat hippocampal formation. Neuroscience 1997;80:1041–1055. [PubMed: 9284059]

Kodam A, Vetrivel KS, Thinakaran G, Kar S. Cellular distribution of gamma-secretase subunit nicastrin in the developing and adult rat brains. Neurobiol Aging 2008;29:724–738. [PubMed: 17222950]

Nadler JV, Perry BW, Gentry C, Cotman CW. Degeneration of hippocampal CA3 pyramidal cells induced by intraventricular kainic acid. J Comp Neurol 1980;192:333–359. [PubMed: 7400401]

Parent AT, Barnes NY, Taniguchi Y, Thinakaran G, Sisodia SS. Presenilin attenuates receptor-mediated signaling and synaptic function. J Neurosci 2005;25:1540–1549. [PubMed: 15703408]

Paxinos, G.; Watson, C. San Diego: Academic Press; 1986. The rat brain in stereotaxic coordinates.

Rojo M, Pepperkok R, Emery G, Kellner R, Stang E, Parton RG, Gruenberg J. Involvement of the transmembrane protein p23 in biosynthetic protein transport. J Cell Biol 1997;139:1119–1135. [PubMed: 9382861]

Simpson JC, Nilsson T, Pepperkok R. Biogenesis of Tubular ER-to-Golgi Transport Intermediates. Mol Biol Cell 2006;17:723–737. [PubMed: 16314391]

Springer S, Chen E, Duden R, Marzioch M, Rowley A, Hamamoto S, Merchant S, Schekman R. The p24 proteins are not essential for vesicular transport in Saccharomyces cerevisiae. Proc Natl Acad Sci U S A 2000;97:4034–4039. [PubMed: 10737764]

Thinakaran G, Borchelt DR, Lee MK, Slunt HH, Spitzer L, Kim G, Ratovitsky T, Davenport F, Nordstedt C, Seeger M, Hardy J, Levey AI, Gandy SE, Jenkins NA, Copeland NG, Price DL, Sisodia SS. Endoproteolysis of presenilin 1 and accumulation of processed derivatives in vivo. Neuron 1996;17:181–190. [PubMed: 8755489]

Thinakaran G, Regard JB, Bouton CML, Harris CL, Price DL, Borchelt DR, Sisodia SS. Stable association of presenilin derivatives and absence of presenilin interactions with APP. Neurobiol Dis 1998;4:438–453. [PubMed: 9666482]

Vassar R. BACE1: the β-secretase enzyme in Alzheimer's disease. J Mol Neurosci 2004;23:105–114. [PubMed: 15126696]

Vetrivel KS, Cheng H, Lin W, Sakurai T, Li T, Nukina N, Wong PC, Xu H, Thinakaran G. Association of γ-secretase with lipid rafts in post-golgi and endosome membranes. J Biol Chem 2004;279:44945–44954. [PubMed: 15322084]

Vetrivel KS, Gong P, Bowen JW, Cheng H, Chen Y, Carter M, Nguyen PD, Placanica L, Wieland FT, Li YM, Kounnas MZ, Thinakaran G. Dual roles of the transmembrane protein p23/TMP21 in the

modulation of amyloid precursor protein metabolism. Mol Neurodegener 2007;2:4. [PubMed: 17288597]

Vetrivel KS, Zhang YW, Xu H, Thinakaran G. Pathological and physiological functions of presenilins. Mol Neurodegener 2006;1:4. [PubMed: 16930451]

Wen C, Greenwald I. p24 proteins and quality control of LIN-12 and GLP-1 trafficking in Caenorhabditis elegans. J Cell Biol 1999;145:1165–1175. [PubMed: 10366590]

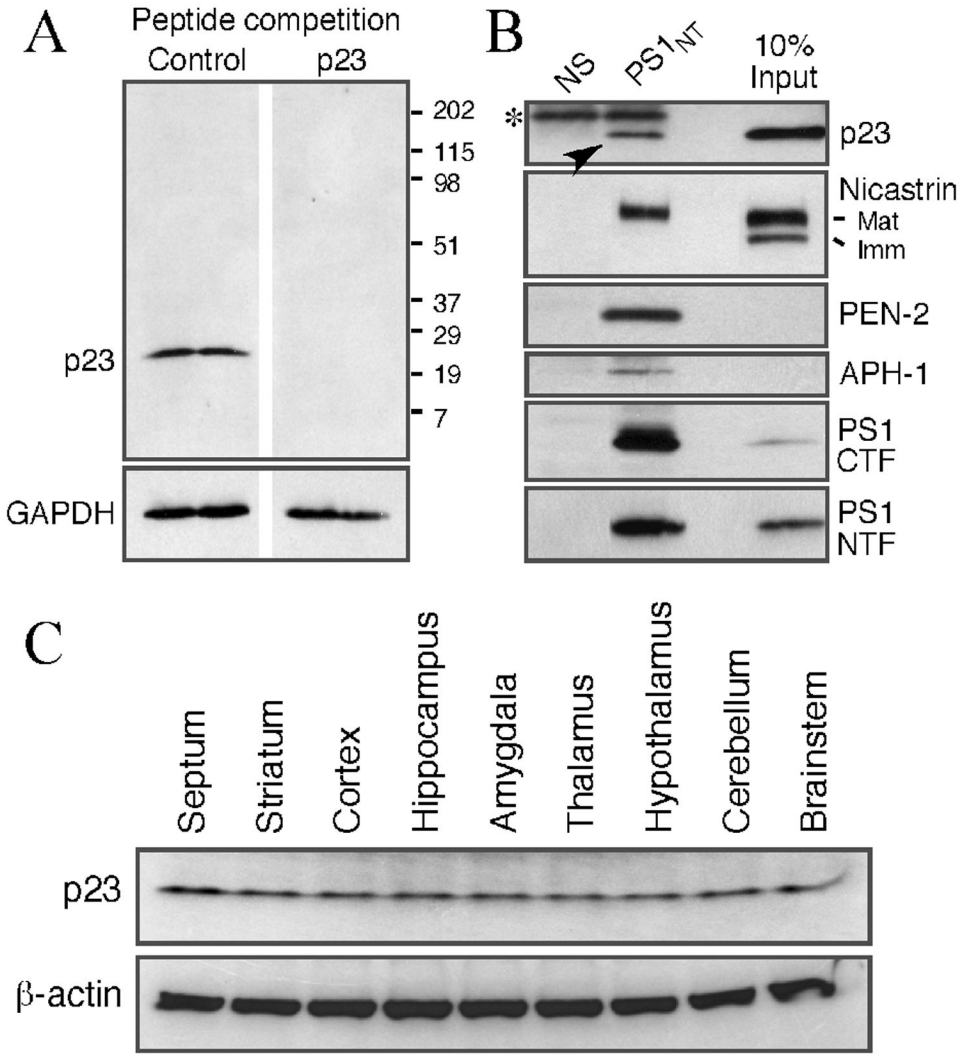

Fig. 1. Western blot analysis of p23 expression in adult brain

(**A**) Characterization of p23 antibody. Western blot of total lysates from mouse N2a neuroblastoma cells probed with p23 antibody pre-incubated with saturating concentrations of unrelated peptide (Control) or the p23 peptide immunogen (p23). (**B**) Co-immunoprecipitation of endogenous p23 with γ-secretase complex. N2a cells were lysed in a buffer containing 1% CHAPSO and aliquots of lysates (300 μg protein) were incubated with a non-specific polyclonal (NS) or PS1 antibody ($PS1_{NT}$). The resulting immunoprecipitates and total lysates corresponding to 10% of the input were probed sequentially with antibodies against p23, nicastrin, PEN-2, APH-1, and PS1 ($PS1_{NT}$ and α-PS1Loop). *Arrowhead* indicates p23 co-immunoprecipitated by PS1 antibody. (**C**) Immunoblot analysis of p23 in different regions of the adult rat brain. The blot was reprobed with an antibody against β-actin as the loading control.

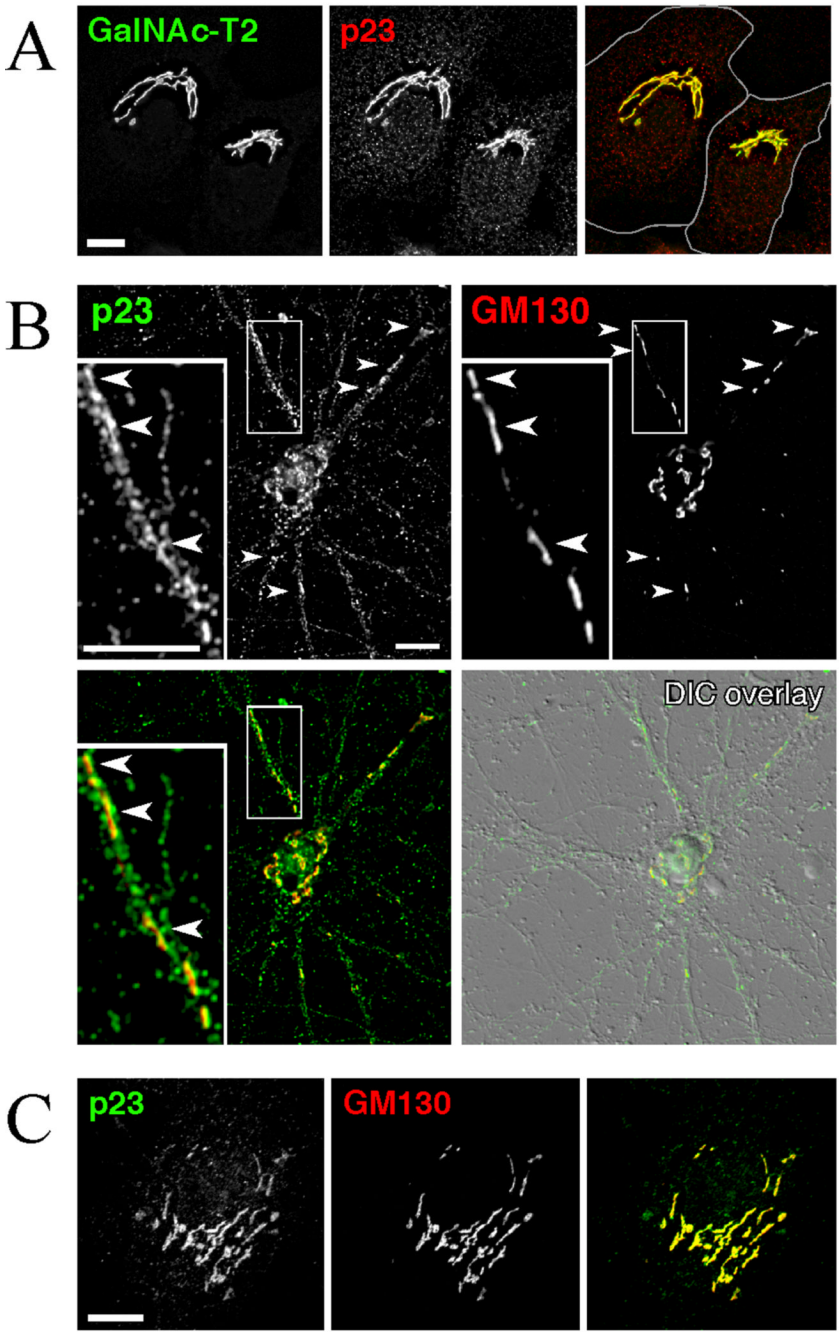

Fig. 2. Immunofluorescence localization of endogenous p23 in HeLa cells, cortical neurons and astrocytes

(A) HeLa cells stably expressing GFP-tagged N-acetylgalactosaminyltransferase-2 were analyzed by immunofluorescence staining with p23 antibody. (**B**) Primary cortical neurons were stained with p23 antibody and a mAb against the cis-Golgi marker GM130. Inserts show higher magnification of the dendritic area indicated by the box. p23 co-localizes with GM130 in the cell body and along the dendrites. *Arrowheads* point to p23 and GM130 co-localization in dendritic Golgi "outposts" (Horton et al., 2005). (**C**) Predominant Golgi localization of p23 in cultured astrocytes. Scale bar = 10 μm.

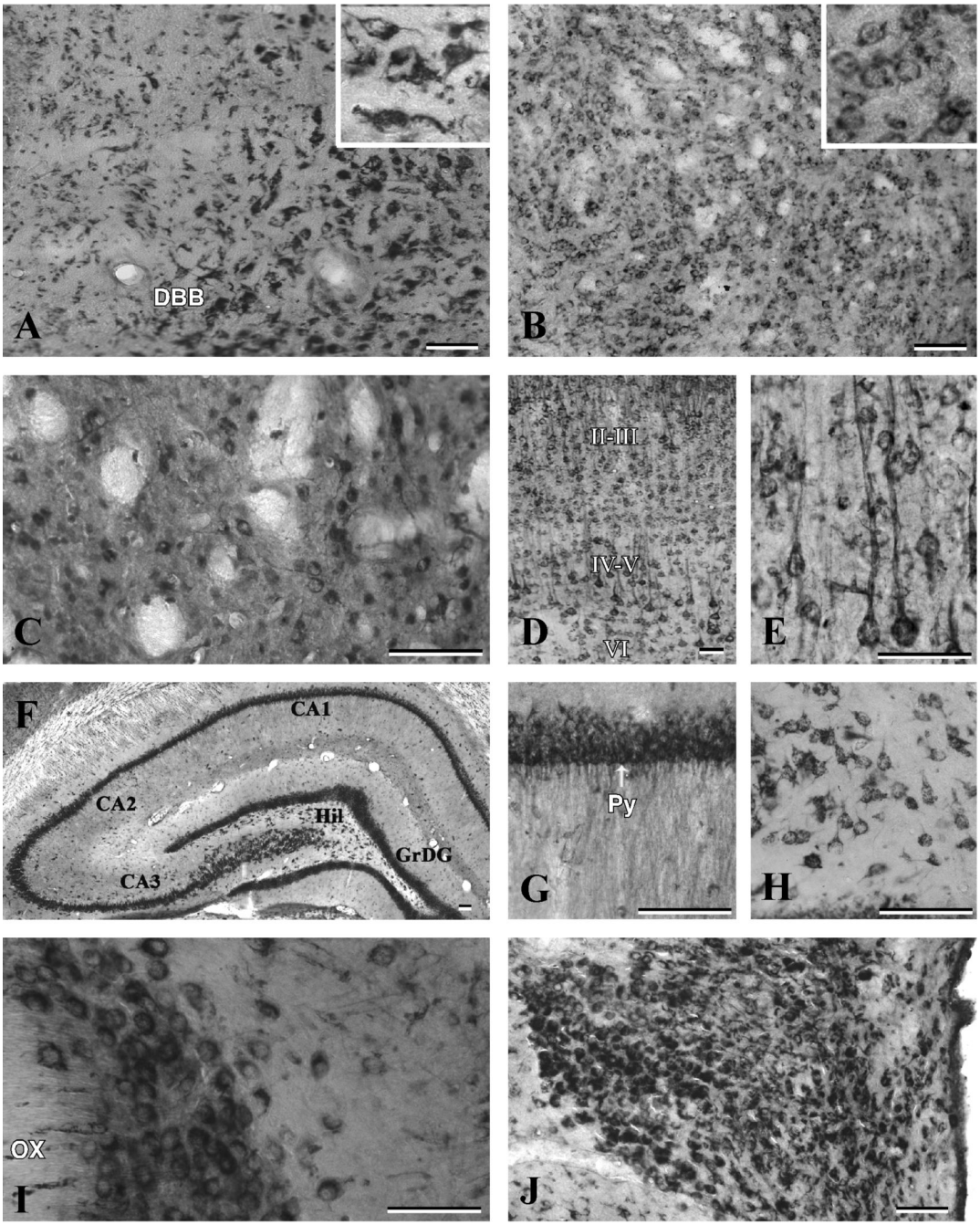

Fig. 3. Photomicrographs of coronal sections of the adult rat brain showing the distribution of p23-immunoreactive neurons and fibers in the diagonal band of Broca

(**A**), globus pallidus (**B**), striatum (**C**), cortex (**D**, **E**), hippocampus (**F**), CA1 pyramidal cell layer of the Ammon's horn (**G**), polymorphic neurons of the hilus (**H**) and supraoptic (**I**) and paraventricular nuclei (**J**) of the hypothalamus. Note that neurons of the diagonal band of Broca, globus pallidus and striatum are moderately labeled, whereas hippocampal pyramidal cell layer and supraoptic as well as paraventricular nuclei exhibit rather strong immunoreactivity. The staining intensity in the neocortex is variable: intense in layers IV–V, moderate in layers II–III and VI and relatively low in layer I. Inset in (**A**) and (**B**) show neuronal labeling at higher

magnification. DBB, diagonal band of Broca; Hil, hilus; GrDG, granular cell layer of the dentate gyrus; Py, pyramidal cell layer; OX, optic chiasma. Scale bar = 50 μm.

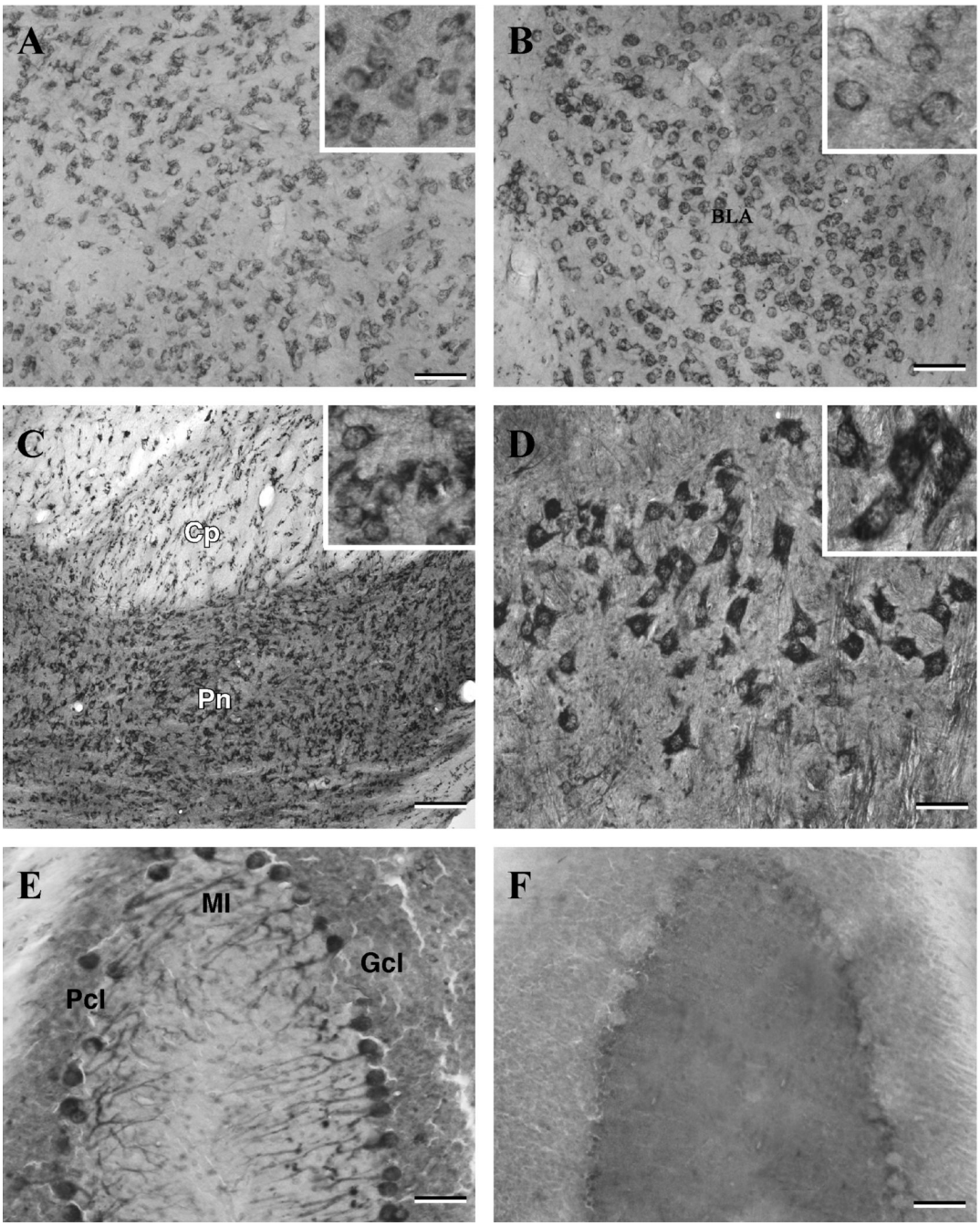

Fig. 4. Photomicrographs of coronal sections of the adult rat brain showing the distribution of p23-immunoreactive neurons and fibers in the medial thalamic nucleus

(**A**), amygdaloid nucleus (**B**), pontine nucleus (**C**), facial nucleus of the brainstem (**D**) and cerebellum (**E**). Note intense labeling of the brainstem neurons and the Purkinje cells of the cerebellum. **F**, represents a cerebellar section processed using the preimmune serum. Insets in (**A–D**) show neuronal labeling at higher magnification. BLA, basolateral amygdale; Cp, cerebral peduncle; Pn, pontine nuclei; Gcl, granular cell layer; Pcl, Purkinje cell layer; Ml, molecular layer. Scale bar = 50 μm.

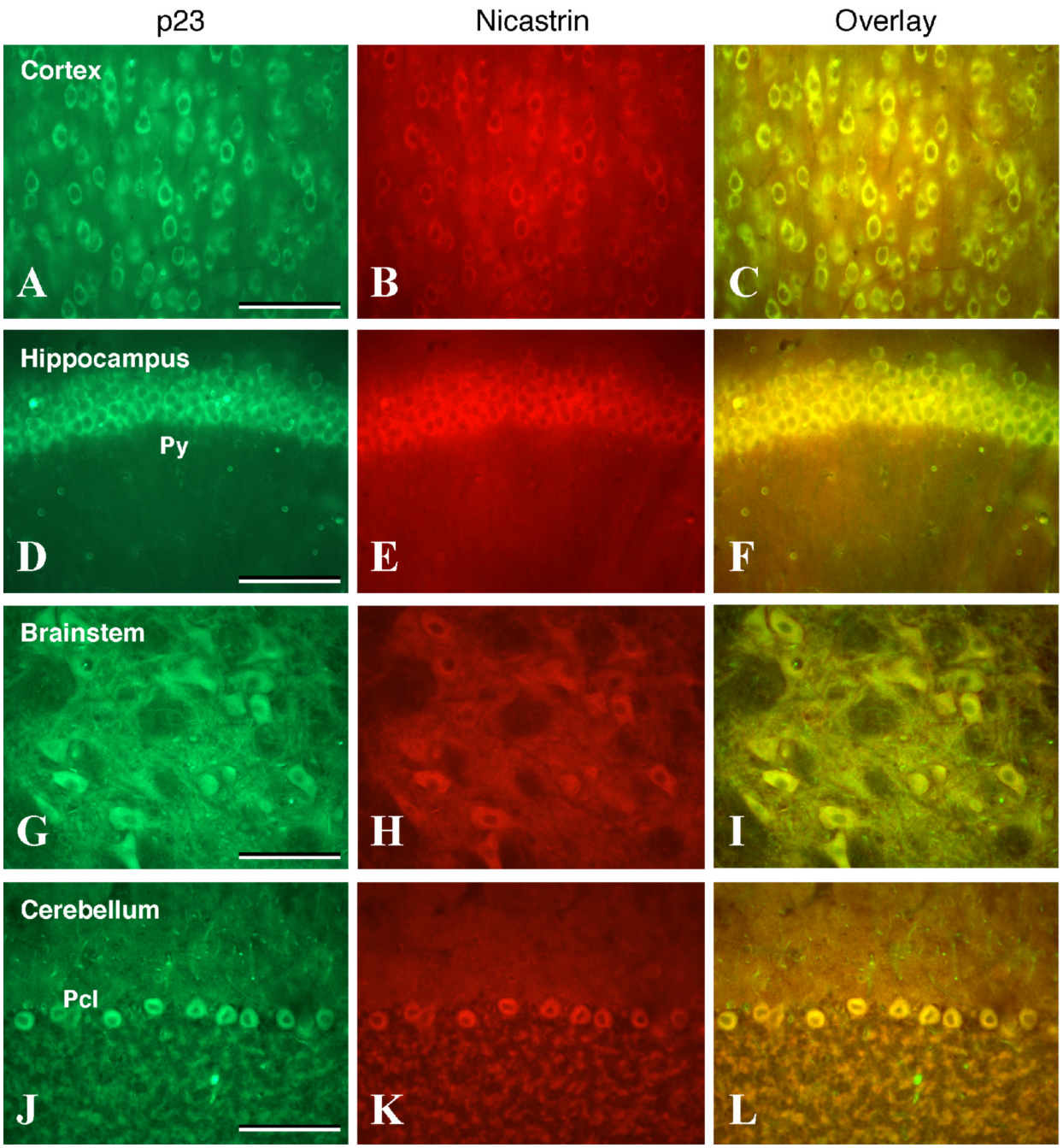

Fig. 5. Double immunofluorescence analysis of p23

(**A**, **D**, **G**, **J**) and nicastrin (**B**, **E**, **H**, **K**) staining in coronal sections of the adult rat brain cortex (**A–C**), hippocampus (**D–F**), brainstem (**G–I**) and cerebellum (**J–L**). Note the widespread coexpression of p23 with nicastrin in all neurons located in the cortex, hippocampal pyramidal cell layer (Py), brainstem motoneurons, and cerebellar Purkinje cells (Pcl). Scale bar = 50 μm.

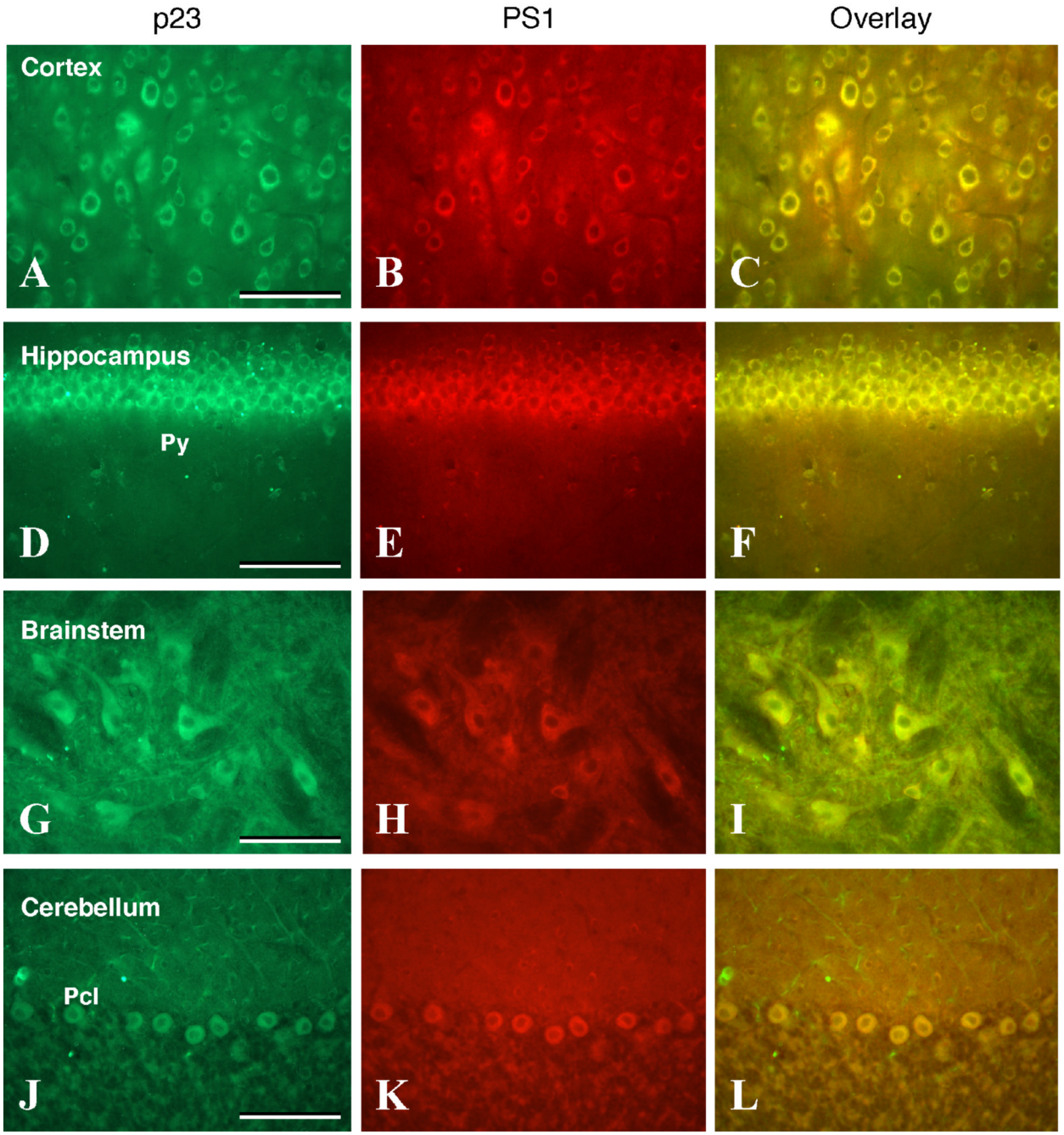

Fig. 6. Double immunofluorescence analysis of p23

(**A**, **D**, **G**, **J**) and PS1 (**B**, **E**, **H**, **K**) staining in adult rat brain cortex (**A–C**), hippocampus (**D–F**), brainstem (**G–I**) and cerebellum (**J–L**). Note the widespread coexpression of p23 with PS1 in all neurons located in the cortex, hippocampal pyramidal cell layer (Py), brainstem motoneurons, and cerebellar Purkinje cells (Pcl). Scale bar = 50 μm.

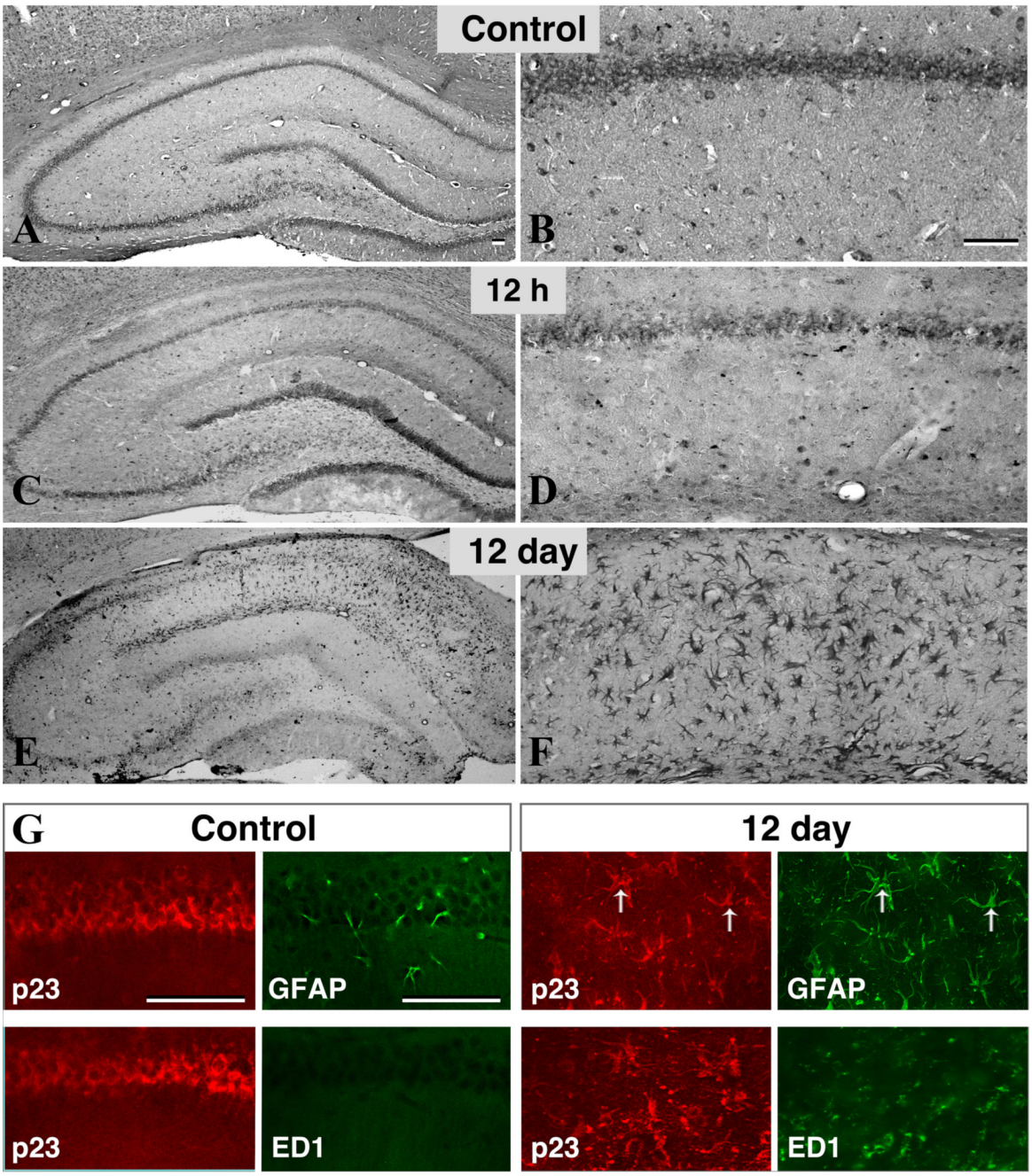

Fig. 7. p23 expression in the brain following kainic acid injury

(**A–F**) The distribution of p23 immunoreactivity in the hippocampal formation (**A**, **C**, **E**) and in the corresponding CA1 sub-field (**B**, **D**, **F**) of control and kainic acid treated rats analyzed 12 h or 12 day following treatment. Note the time-dependent decrease in neuronal and increase in glial p23 immunoreactivity following the administration of kainic acid. (**G**) Double immunofluorescence analysis of p23 expression in GFAP-labeled astrocytes and ED1-positive microglia in rat hippocampus. Note that p23 staining is not evident in control brain astrocytes but is highly expressed in reactive astrocytes 12 days following kainic acid administration. p23 staining is undetectable in ED1-positive microglia in control and kainic acid treated animals. Scale bar = 50 μm.

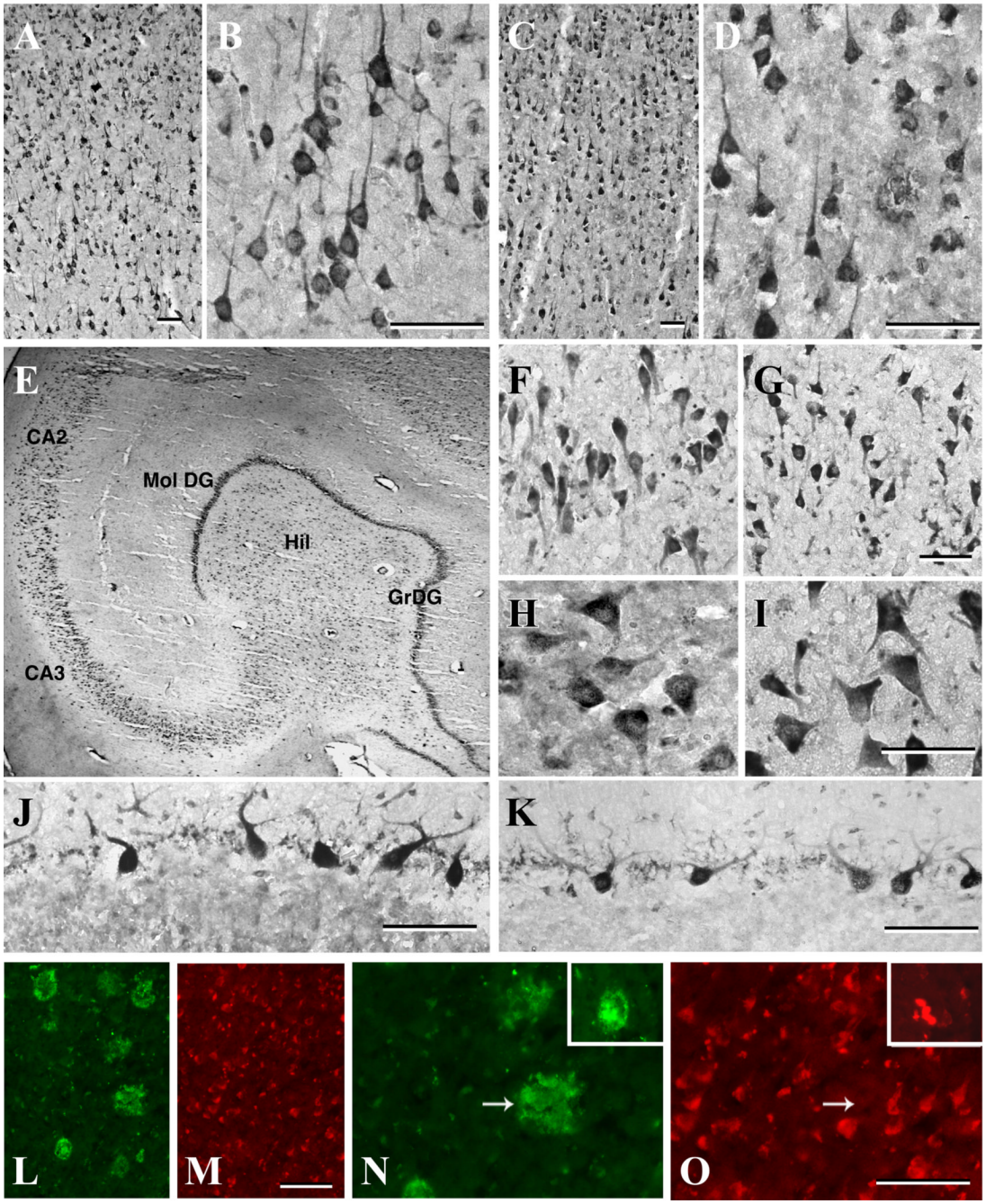

Fig. 8. The distribution of p23 immunoreactivity in human brain

Neurons in the frontal cortex (**A–D**), as well as hippocampal neurons in the pyramidal cell layer (**E**, **F**, **G**), granule cell layer (**E**) and in the hilus (**E**, **H**, **I**) are strongly labeled, whereas cerebellar Purkinje cells (**J**, **K**) are moderately labeled. No marked alteration in the profile of p23 expression was evident in the AD brains (**C**, **D**, **G**, **I**, **K**) compared to age-matched controls (**A**, **B**, **E**, **F**, **H**, **J**). (**L–O**) Double immunofluorescence analysis of Aβ-positive neuritic plaques (**L**, **N**) and p23 expression (**M**, **O**) in the frontal cortex of AD brain. Note the lack of overlap between p23 staining and neuritic plaques, except in rare instances (insert). GrDG, granule cell layer of the dentate gyrus; Mol Dg, molecular layer of the dentate gyrus Hil, hilus. Scale bar = 50 μm.

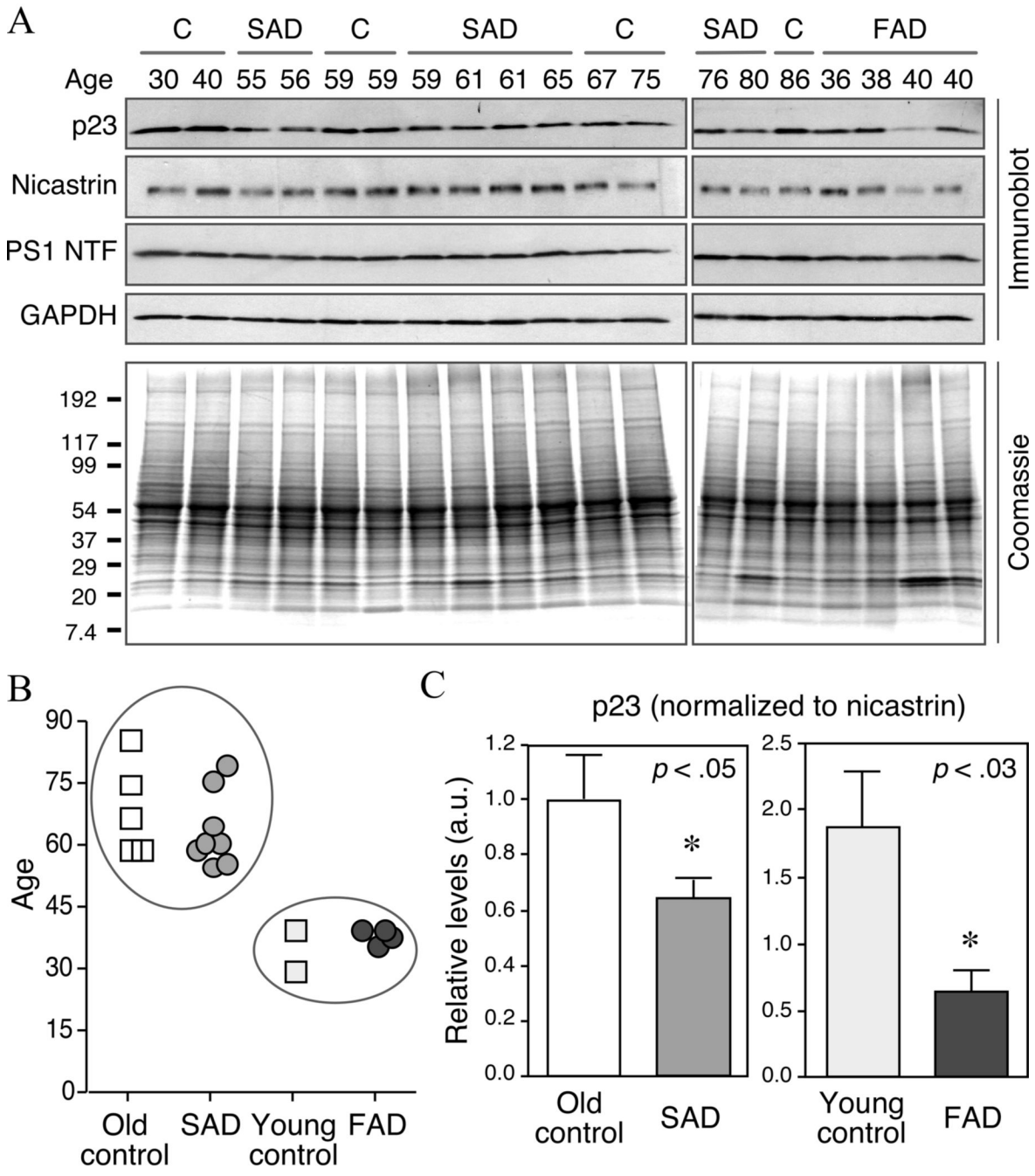

Fig. 9. Immunoblot analysis of p23 expression in human cortical brain extracts

(**A**) Human brain tissue was homogenized in SDS extraction buffer and aliquots of total homogenates were fractionated by SDS-PAGE. The blots were sequentially probed with antibodies against p23, nicastrin, PS1 NTF, and GAPDH. Coomassie stained gels containing aliquots of homogenates is shown in the bottom panel. *C*, control brains, free of neurological diseases; *SAD*, sporadic AD brains; *FAD*, familial early-onset AD patients harboring *PSEN1* mutations. (**B**) The age at death of all individuals is plotted and also indicated on top of each lane in the gel in panel A. The circles enclose SAD patients (mean age 64.13 ± 3.2) and age-matched old controls (mean age 69.2 ± 5.1), as well as FAD patients (mean age 38.5 ± 1) and young controls (mean age 35 ± 5). (**C**) Signal intensities of p23 and nicastrin were quantified

and the ratios of p23 to nicastrin signal intensity in SAD or FAD relative to their respective age-matched controls were plotted. Note that for easier comparison between SAD and FAD in these plots, all values were normalized to old controls.

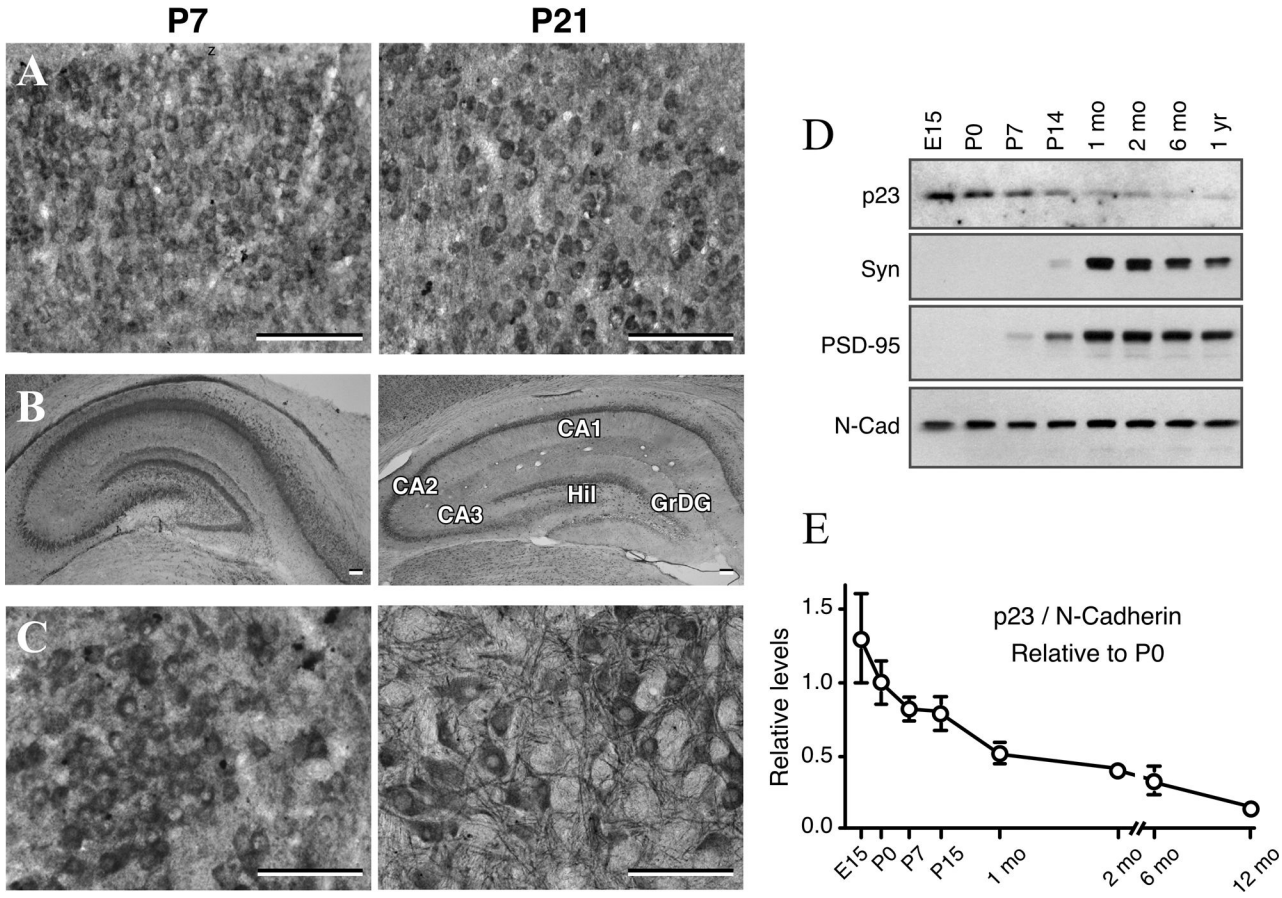

Fig. 10. Expression of p23 during postnatal development

Immunohistochemical staining showing the levels and expression of p23 in the cortex (**A**), hippocampus (**B**) and brainstem (**C**) of the postnatal rat brains at postnatal day 7 and 21. Note the relatively stronger p23 staining of neuronal cell bodies at P7 (left panels in **A–C**), and readily apparent staining of neuronal processes at P21 postnatal brains (right panels in **A–C**). Hil, hilus; GrDG, granular cell layer of the dentate gyrus. Scale bar = 50 μm. (**D** and **E**) Immunoblot analysis of p23 expression during postnatal brain development. Mouse brains harvested at the indicated stages of embryonic and postnatal development and adult were separated on SDS-PAGE and analyzed by immunoblotting. Note the high embryonic expression of p23 that gradually declines after birth. Signal intensities of p23 was quantified from analysis of three or more animals and normalized to N-cadherin levels. For comparison, the normalized expression level of each protein at embryonic stage P0 was set to 1 and the level of expression relative to P0 was plotted.

Table 1

Quantification of steady-state p23 levels in SAD, FAD, and respective age-matched controls

	p23 (normalized to nicastrin signal)	p23 (normalized to GAPDH signal)	nicastrin (normalized to GAPDH signal)
Age-matched controls *versus* SAD	64.50 ± 7.0**	62.85 ± 9.4**	95.07 ± 9.8
Age-matched controls *versus* FAD	34.16 ± 8.5***	36.07 ± 11.3***	89.50 ± 20.0

The normalized steady-state levels of p23 and nicastrin in SAD and FAD patients are shown as mean ± SEM relative to controls (see Fig. 9B for details).

** $p<0.05$

*** $p<0.03$ in comparison to respective age-matched controls. The levels of nicastrin were not significantly different between AD and controls.